

Equilibria and dynamics of liquid-phase trinitrotoluene adsorption on granular activated carbon: Effect of temperature and pH

Jae-Wook Lee^a, Tae-Hoon Yang^a, Wang-Geun Shim^b, Tae-Ouk Kwon^c, Il-Shik Moon^{c,*}

^a Department of Environmental and Chemical Engineering, Seonam University, Namwon 590-711, Republic of Korea

^b Faculty of Applied Chemistry, Chonnam National University, Gwangju 500-757, Republic of Korea

^c Department of Chemical Engineering, Sunchon National University, Suncheon 540-742, Republic of Korea

Received 19 February 2006; received in revised form 25 June 2006; accepted 28 June 2006

Available online 1 July 2006

Abstract

Environmental regulations for removal of trinitrotoluene (TNT) from wastewater have steadily become more stringent. This study focuses on the adsorption equilibrium, kinetics, and column dynamics of TNT on heterogeneous activated carbon. Adsorption equilibrium data obtained in terms of temperature (298.15, 313.15 and 323.15 K) and pH (3, 8 and 10) were correlated by the Langmuir equation. In addition, the adsorption energy distribution functions which describe heterogeneous characteristics of porous solid sorbents were calculated by using the generalized nonlinear regularization method. Adsorption breakthrough curves were studied in activated column under various operating conditions such as temperature, pH, concentration, flow rate, and column length. We found that the effect of pH on adsorption breakthrough curves was considerably higher than other operating conditions. An adsorption model was formulated by employing the surface diffusion model inside the activated carbon particles. The model equation that was solved numerically by an orthogonal collocation method successfully simulated the adsorption breakthrough curves. © 2006 Elsevier B.V. All rights reserved.

Keywords: Trinitrotoluene; Heterogeneous activated carbon; Dynamics; Operating conditions

1. Introduction

Environmental regulations have steadily become more stringent for the removal of trinitrotoluene (TNT) from wastewater and groundwater [1]. Moreover, the low discharge limit of 1 ppm of TNT wastewater is generally required [2]. However, the conventional treatment techniques have been found unsuitable for the reduction of the low discharge limit required. Thus, many removal methods such as incineration, biodegradation, catalytic oxidation, solvent extraction, and carbon adsorption have been investigated [3–5]. Among them, adsorption on granular activated carbon has been employed in some of the US military establishments.

Recently, Marinovic et al. [1] have studied the effect of operating parameters (i.e., temperature, concentration, flow rate, and column length) on the dynamic adsorption of TNT on granular activated carbon. They employed three adsorption dynamic models (i.e., model of normal distribution; model of a first order

system with dead time; model based on gas adsorption kinetics) to simulate the breakthrough curves. However, the dynamic models that do not take the adsorption equilibrium into consideration seem to be very limited for the analysis of the practical adsorption process. To overcome the limitation, therefore, a general and more realistic adsorption dynamic model based on the thermodynamic and kinetic approaches is required. Muralidharan et al. [6] have investigated the adsorption and desorption characteristics of explosive vapors for the design of sensors. More recently, Rajagopal and Kapoor [2] have examined the dynamic adsorption characteristics of nitro-organics (TNT, dinitrotoluene, nitrobenzene) in bench-scale activated carbon column to understand their dynamic adsorption behavior for dilute aqueous solutions.

Adsorption separation processes are generally carried out in fixed-bed adsorbers which contain porous adsorbent particles. The performance of an adsorption-based separation process depends much on the effectiveness of design and operating conditions. The shape and width of the adsorption breakthrough curve are important in designing adsorbers. The breakthrough curve generally depends on the adsorption isotherm and the transport mechanisms in sorbent particles as well as in operat-

* Corresponding author. Tel.: +82 61 750 3581; fax: +82 61 750 3580.
E-mail address: ismoon@sunchon.ac.kr (I.-S. Moon).

Nomenclature

A	surface area of sorbent particles (m^2)
b	Langmuir constant ($\text{m}^3 \text{mol}^{-1}$)
c_{sol}	solubility of adsorbate (mol m^{-3})
C	concentration in the fluid phase (mol m^{-3})
D	column diameter (m)
D_L	axial dispersion coefficient ($\text{m}^2 \text{s}^{-1}$)
D_m	molecular diffusion coefficient ($\text{m}^2 \text{s}^{-1}$)
D_s	surface diffusion coefficient ($\text{m}^2 \text{s}^{-1}$)
E	percent error (%)
E_{12}	energy difference of components
F	energy distribution function
k_f	film mass transfer coefficient (m s^{-1})
L	column length (m)
N	number of data point
q	concentration in particle phase (mol kg^{-1})
q_m	Langmuir constant (mol kg^{-1})
r	radial distance (m)
R	particle radius (m)
t	time (s)
T	temperature (K)
V	volume of batch adsorber (m^3)
w	sorbent weight (kg)
x	mole fraction in adsorbed phase
z	axial distance (m) or mole fraction

Greek letters

ε_b	bed porosity
Φ	ratio of the molecular partition functions for the surface and bulk solutions
θ_T	total fractional coverage
ρ_p	particle density (kg m^{-3})
ν	interstitial velocity (m s^{-1})
ω	c/c_{sol}

ing conditions of the column [7–9]. Unfortunately, experimental and theoretical studies of the equilibrium and column dynamics of TNT on activated carbon have been very limited to date.

The goal of our work is to develop a cost-effective removal process of TNT dissolved in water by using adsorption-based technology. For this purpose, experimental and theoretical studies on the adsorption equilibrium, kinetics, and column dynamics of TNT were systematically investigated in a small-scale activated carbon column. Moreover, a simple dynamic model was constructed by employing the adsorption equilibrium and the surface diffusion model for intraparticle mass transport to simulate adsorption breakthrough curves obtained under the key operating conditions such as temperature, pH, flow rate, concentration, and column length. On the other hand, adsorption energy distribution functions of TNT on heterogeneous activated carbon obtained as functions of temperature and solution pH were calculated on the basis of a generalized nonlinear regularization method since the surface energy heterogeneity offers the fundamental and informative data required in understanding the adsorption properties [10–12].

2. Theoretical approach

2.1. Adsorption model

A fixed-bed adsorption model was developed to analyze and simulate the column dynamics under important operating conditions. The underlying assumptions in developing the model equations are that:

1. the adsorber operates isothermally;
2. the bulk concentration of adsorbate is uniform in an adsorber;
3. the adsorbents are spherical particles with an identical radius;
4. the physical properties of the adsorbent and the column wall are constant;
5. radial concentration and velocity gradients within the bed are negligible;
6. external and internal mass transport resistances are included;
7. the flow through a fixed bed is axially dispersed.

Applying the above assumptions to the mass balance of the liquid phase through the bed, the following governing equation was obtained:

$$-D_L \frac{\partial^2 C}{\partial z^2} + \nu \frac{\partial C}{\partial z} + \frac{\partial C}{\partial t} + \frac{1 - \varepsilon_b}{\varepsilon_b} \frac{3k_f}{R} (C - C_s) = 0 \quad (1)$$

The initial and boundary conditions are

$$C(z, t = 0) = 0 \quad (2)$$

$$D_L \frac{\partial C}{\partial z} \Big|_{z=0} = -\nu(C|_{z=0^-} - C|_{z=0^+}) \quad (3)$$

$$\frac{\partial C}{\partial z} \Big|_{z=L} = 0 \quad (4)$$

Assuming that surface diffusion is the dominant mechanism of the intraparticle mass transfer, adsorbate diffusion within a particle is described by

$$\frac{\partial C}{\partial t} = D_s \left(\frac{\partial^2 q}{\partial r^2} + \frac{2}{r} \frac{\partial q}{\partial r} \right) \quad (5)$$

with the following initial and boundary conditions:

$$q(r, t = 0) = 0 \quad (6)$$

$$\frac{\partial q}{\partial r} \Big|_{r=0} = 0 \quad (7)$$

$$D_s \rho_p \frac{\partial q}{\partial r} \Big|_{r=R} = k_f (C - C_s) \quad (8)$$

2.2. Numerical solution

The system of equations for both interparticle and intraparticle mass balance, i.e., Eqs. (1) and (5) were solved numerically by applying the orthogonal collocation to discretize the two equations [13]. The discretization was done for the spatial variable, resulting in a set of ODEs with the adsorbate concentrations

Table 1
Activated carbon properties

Particle size, mean diameter (μm)	825
Particle density (m^3/kg)	810
Particle porosity	0.55
Moisture holding capacity (%)	5
Surface area BET– N_2 (m^2/g)	1170
Average pore diameter (\AA)	32
Average pore volume (cm^3/g)	0.65

as the dependant variable. These equations are solved on a personal computer using a FORTRAN Compiler in double precision and using LSODI of the international mathematics and science library (IMSL). Details of the collocation form of the equations as well as the solution scheme, are discussed elsewhere [9,14].

3. Experimental

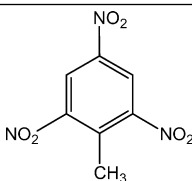
3.1. Materials

The adsorbent used in this study was activated carbon supplied by Dongyang Co. (Korea). For the equilibrium isotherm experiment, the adsorbent was sieved to give the fraction of 14/30 mesh particle size. All particles were boiled in distilled water for 12 h, dried at 373.15 K thermostatic oven, and kept on a desiccator. The nitrogen adsorption apparatus (Micromeritics, model ASAP-2010) measured the surface area and pore size distribution. The surface area was found to be large about $1170 \text{ m}^2/\text{g}$. The physical properties of activated carbon are listed in Table 1. All experiments were carried out with the solutions of TNT (from industrial production) in distilled water. The important physical properties of TNT are listed in Table 2.

3.2. Procedure

The equilibrium data were obtained by introducing a given amount of activated carbon (i.e., 0.5 g) into an aqueous solution of TNT with a known concentration (within the range of 1–50 mg/L), shaking the adsorbate in a constant temperature

Table 2
Properties of TNT

Chemical structure	
Chemical formula	$\text{C}_7\text{H}_5\text{N}_3\text{O}_6$
MW	227.13
Color	Yellow-white
Odor	Odorless
Solubility at 20 °C (mg/L)	130
Melting point (°C)	80.1
Boiling point (°C)	240
Partition coefficients, $\log K_{ow}$	1.60
Vapor pressure at 20 °C (atm)	2.618×10^{-2}
Henry's law constant at 20 °C ($\text{atm m}^3/\text{mol}$)	4.57×10^{-7}

incubator sufficiently for 72 h until the equilibrium was reached. The adsorption capacity of TNT was determined from material balance by measuring the remaining TNT concentration in the solution. To obtain concentration decay curves, batch experiments were conducted in a carberry-type batch adsorber of $1.0 \times 10^{-3} \text{ m}^3$. Sorbent particles were loaded into four cages made of stainless-steel screen and the cages were affixed to the rotating shaft to permit good contact with the solution. All the experiments were carried out at approximately 300 rpm under varying temperatures (298.15, 313.15 and 323.15 K) and pH (3, 8 and 10). Fixed-bed adsorption experiments were carried out in an adsorber made of a glass column of 2.5 cm in diameter and 25 cm in length (Fig. 1). The column was lined with a water jacket to maintain a uniform column temperature, and all the experiments were performed under varying temperatures (298.15, 313.15 and 323.15 K) and pH (3 and 8). A precision FMI pump (model RHOCKE) regulated the flow rate. The solution was introduced downward into the column. To prevent channeling and to enhance a uniform flow, small glass beads were packed in both the top and bottom regions of the column.

3.3. Analysis

The concentration of TNT in the solution was analyzed by a Shimadzu model LC-6AD HPLC system (Japan) equipped with a UV detector at 254 nm and Eurospher RP-18 (Fa. Knauer, Berlin, Germany) under the flow rate of 1.5 ml/min and at 303.15 K. Deionized water, analytical grade methanol, and acetonitrile were mixed at a ratio of 50:38:12 (v/v), filtered, and degassed to use as a mobile phase.

4. Results and discussion

4.1. Equilibrium study

Adsorption equilibrium is the most fundamental data on an adsorption system. It is also very important in model prediction for analyzing and designing an adsorption process. Fig. 2a and b show the adsorption isotherms in terms of temperature (298.15, 313.15 and 323.15 K) and pH (3, 8 and 10). The adsorption capacity increased with increasing temperature (Fig. 2a), which indicates chemisorption. The rate of adsorption is an important criterion for the determination between physisorption and chemisorption. The chemisorption usually requires activation energy which increases with increasing temperature. Similar results have been reported by Marinovic et al. [1]. They investigated the adsorption capacity of activated carbon under wide temperature ranges from 283.15 to 333.15 K. At temperatures up to 293.15 K, physical adsorption predominates while the contribution of chemisorption becomes increasingly large within the temperature region from 298.15 to 333.15 K because of the positive temperature coefficient of the rate of chemisorption [1]. On the other hand, Fig. 2b shows the adsorption isotherms in terms of pH (3, 8 and 10). As expected, the adsorption capacity increased with decreasing pH (i.e., increasing hydrogen concentration) and the isotherm data showed more concave (i.e., favorable adsorption). To compare the influence of tempera-

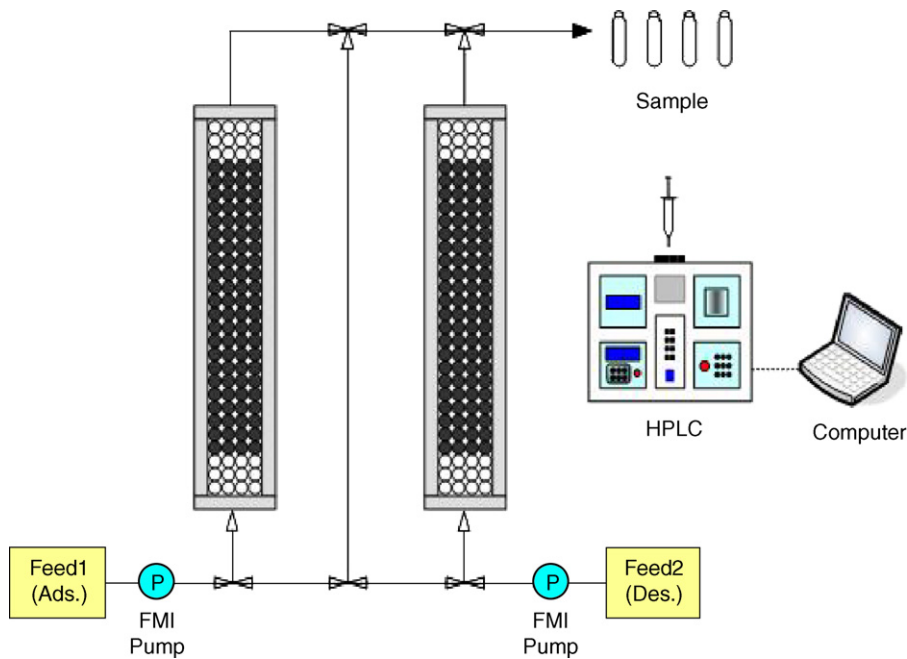


Fig. 1. Schematic diagram of fixed-bed apparatus.

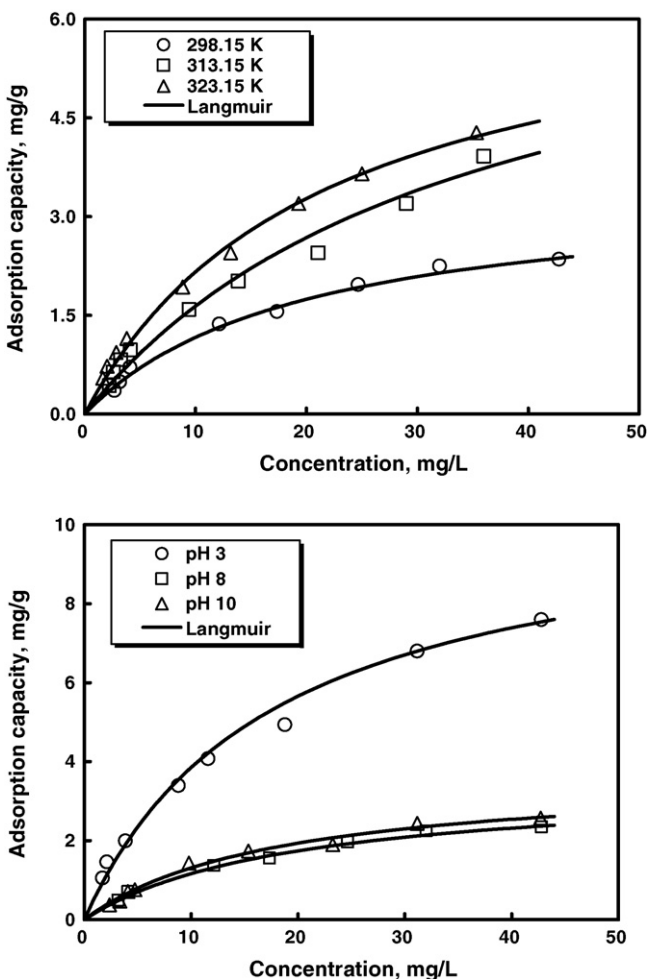


Fig. 2. Adsorption isotherm of TNT in terms of: (a) temperatures at pH 8 and (b) pH at 298.15 K.

ture on adsorption capacity as a function of solution pH, the adsorption isotherm data at pH 3 were obtained under higher temperatures (313.15 and 323.15 K). As a result, the adsorption capacity greatly increased at lower pH. In addition, the effect of pH on the adsorption capacity was much higher than that of temperature. This result implies that the effective separation of TNT was achieved at lower pH and higher temperature.

Adsorption equilibrium data of TNT on activated carbon were correlated with the Langmuir equation:

$$\text{Langmuir } q = \frac{q_m b C}{1 + b C} \tag{9}$$

The parameters were obtained by fitting the data using a modified Levenberg–Marquart method (IMSL routine DUNSLF). The object function, $E(\%)$, represents the average percent deviation between experimental and predicted results as follows:

$$E(\%) = \frac{100}{N} \sum_{k=1}^N \frac{|q_{\text{exp},k} - q_{\text{cal},k}|}{q_{\text{exp},k}} \tag{10}$$

The solid lines in Figs. 2 and 3 are the results predicted by Langmuir parameters (Table 3).

4.2. Adsorption energy distribution

It has been well known that the porous media have different structural and chemical properties. Thus, the adsorption properties of adsorbents are very complex and highly dependent on the adsorption systems consisting of the adsorbate and the adsorbent. Adsorption energy distributions have been extensively applied for characterizing the numerous adsorption systems and understanding the surface energy heterogeneities. The fundamental adsorption integral equation of the dilute solutions on

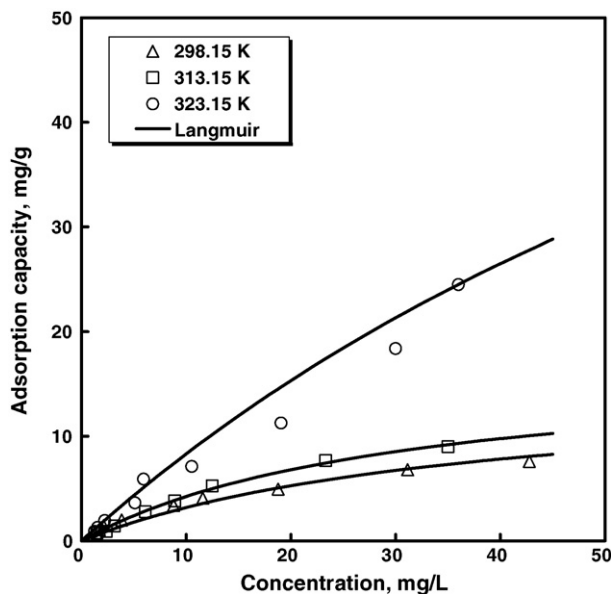


Fig. 3. Adsorption isotherm of TNT in terms of temperatures at pH 3.

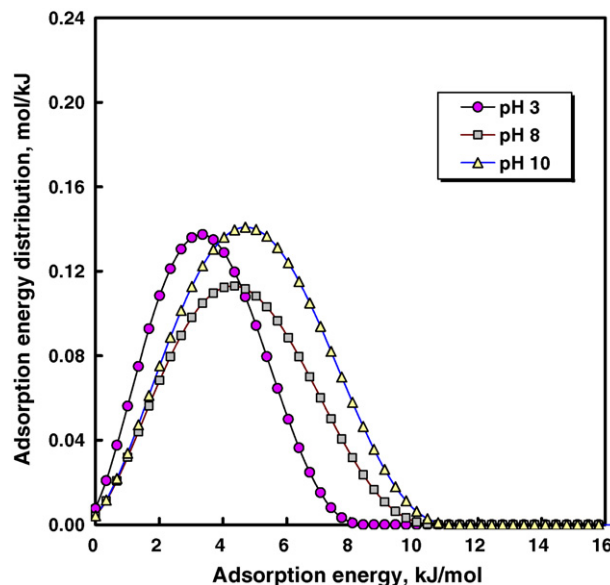


Fig. 4. Adsorption energy distributions of TNT on heterogeneous activated carbon in terms of solution pH.

energetically heterogeneous solid surfaces is given as follows:

$$\theta_T = \int_{E_{12min}}^{E_{12max}} \frac{\Phi \omega \exp(E_{12}/RT)}{1 + \Phi x \exp(E_{12}/RT)} F(E_{12}) dE_{12} \quad (11)$$

where θ_T is the total fractional coverage, E_{12} is the energy difference of components, $\Phi = \Phi(c, \theta_T)$ is a model dependent function (i.e., ratio of the molecular partition functions for the surface and bulk solutions), $F(E_{12})$ is the energy distribution function, ω is the relative concentration, R is the gas constant, and T is the absolute temperature. This is the well-known linear Fredholm integral equation of the first kind and the calculation of adsorption energy distribution is an ill posed problem. For the current work, we investigated the generalized nonlinear regularization method based on smoothness constraint (i.e., Tikhonov regularization) and edge preserving regularization methods. The generalized nonlinear regularization method can avoid the difficulties that result from the ill-posed nature of an adsorption integral equation [11].

The proper selection of adsorption isotherm equation for the calculation of energy distribution is very important in analyzing the heterogeneous adsorption systems. In general, Langmuir isotherm has been extensively used to determine the monolayer

amount in aqueous adsorption systems. However, Podkoscielny et al. [12] have reported that the Langmuir–Freundlich isotherm equation could be more reasonable for estimating the monolayer capacity of liquid sorption and correlating experimental adsorption data. In addition, Langmuir–Freundlich equation seems to be suitable for approximating the most adsorption systems having quasi-Gaussian energy distribution to describe the adsorption isotherm data and surface heterogeneity. Therefore, the Langmuir–Freundlich isotherm parameters ($q_m = 20.747$, $b = 0.011$, $n = 0.697$ for pH 3; $q_m = 3.416$, $b = 0.015$, $n = 0.739$ for pH 8; $q_m = 4.493$, $b = 0.035$, $n = 0.882$ for pH 10) were used in the present study. The adsorption energy distribution curves of TNT for different pH exhibited single peaks (Fig. 4). The highest adsorption energy peaks (i.e., around 0.135 mol/kJ) for pH 3 and 10 were observed at adsorption energy 3 kJ/mol for pH 3 and 5 kJ/mol for pH 10. Low energy peak (i.e., 0.11 mol/kJ) was observed at adsorption energy 4 kJ/mol for pH 8. The shape and the intensity of the adsorption energy distribution curve were highly related with the microporosity of the adsorbent. In general, the activated carbon with a relatively large surface area and a small pore size possesses a wide range of adsorption energy. Contrary to our expectation, the adsorption of TNT on the activated carbon in terms of different pH seems to be a nearly homogenous adsorption based on the results of the shape and intensity of the adsorption energy distribution.

Table 3
Adsorption isotherm parameters of TNT on different adsorbents at 298.15 K

Temperature (K)	pH	Parameters	
		q_m	b
298.15	8	3.459	5.078×10^{-2}
313.15	8	7.329	2.886×10^{-2}
323.15	8	6.765	4.691×10^{-2}
298.15	3	10.650	5.664×10^{-2}
298.15	10	3.697	5.499×10^{-2}
313.15	3	17.310	3.239×10^{-2}
323.15	3	97.805	9.288×10^{-3}

4.3. Kinetic study

It is important to estimate the values of the solution-particle mass transfer resistance and the internal mass transfer when highly porous adsorbents are used. Especially, the determination of diffusion coefficients is an important task since intraparticle diffusion is usually the rate-controlling step in most adsorp-

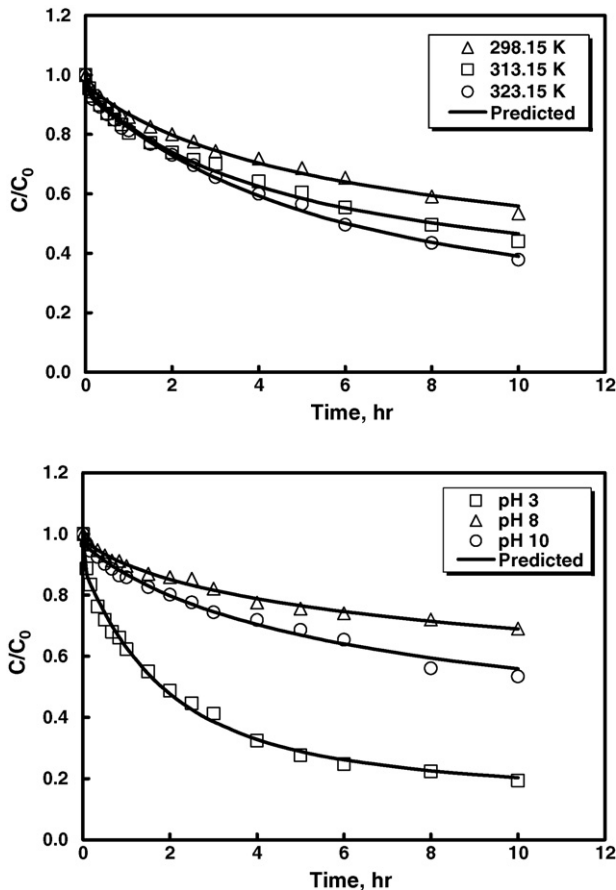


Fig. 5. Concentration decay curves of TNT in terms of: (a) temperatures at pH 8 and (b) pH at 298.15 K (fixed conditions: $w = 5.0$ g, $V = 1$ L, $C_0 = 7.35$ mg/L).

tion processes. Intraparticle diffusion within porous sorbents depends on the mechanism of adsorbate transport, namely, pore diffusion, surface diffusion, and others. In this work, the surface diffusion model was employed. Among the various methods of determining the diffusion coefficient in the literature, the most general method for this is to compare the experimental concentration history and the predicted result by using a specified diffusion model. The experimental and predicted concentration decay curves of TNT are shown in Fig. 5. The solid line is the result predicted by using the surface diffusion model (Eq. (5)). The external and effective surface diffusion coefficients determined are in the range of $(1.17\text{--}8.57) \times 10^{-6}$ m s $^{-1}$ and $(3.17\text{--}5.50) \times 10^{-13}$ m 2 s $^{-1}$ under the various experimental conditions of temperatures and pH (Table 4).

Table 4
External and internal mass transfer coefficients in terms of temperature and pH

Temperature (K)	pH	k_f (m s $^{-1}$)	D_s (m 2 s $^{-1}$)
298.15	8	8.57×10^{-6}	5.50×10^{-13}
313.15	8	1.18×10^{-6}	4.95×10^{-13}
323.15	8	1.17×10^{-6}	3.17×10^{-13}
298.15	3	3.16×10^{-6}	4.98×10^{-13}
298.15	10	7.57×10^{-6}	5.35×10^{-13}

4.4. Column dynamics in fixed-beds

As a piece of commercial equipment for adsorption separation, a column adsorber has been used since it gives a sharp breakthrough by means of the difference in affinity to the particle. The breakthrough curve of all the species in general depends on the adsorption equilibrium, the interparticle mass transfer, and the hydrodynamic conditions in the column. These factors tend to make the breakthrough curves more dispersive or less sharp. Recently, Marinovic et al. [1] have compared the adsorption dynamic models ((a) a model of normal distribution; (b) a model of a first order system with dead time; (c) a model based on gas adsorption kinetics) for describing the experimental results of the dynamic adsorption of TNT by activated carbon. Although the models employed are simple because of no consideration of adsorption isotherm, their limitations made them unsuitable for the analysis of the practical adsorption process operated under wide experimental conditions. Therefore, it is reasonable to consider the adsorption equilibrium and the mass transport simultaneously in simulating the adsorption behavior in the fixed-bed adsorber.

In the columns packed with porous adsorbents, the main parameters for the transport of adsorbates are the axial dispersion coefficient, the external film mass transfer coefficient, and the intraparticle diffusion coefficient. The axial dispersion contributes to the broadening of the adsorption front because of the contribution of molecular diffusion and the dispersion caused by fluid flow. A correlation of axial dispersion suggested by Wakao and Funazkri [8] has been used successfully for liquid-phase systems:

$$D_L = \left[\frac{20}{Re Sc} + \frac{1}{2} \right] 2\nu R \quad (12)$$

For spherical particles, the external film mass transfer coefficient, k_f in columns, has been correlated by the Ranz and Marshall equation [7]:

$$\frac{2k_f R}{D_m} = 2.0 + 0.6Sc^{1/3} Re^{1/2} \quad (13)$$

where Sc and Re mean Schmidt and Reynolds numbers, respectively. Molecular diffusion coefficient (D_m) of TNT in water was estimated by the Wilke–Chang equation [15]. The average axial dispersion coefficient determined under our experimental conditions was 1.01×10^{-6} m 2 s $^{-1}$. The parameters of diffusion coefficients determined in the previous section were used without further adjustment.

The operational factors such as temperature, pH, input concentration, flow rate and column length are important in column designing and optimization. In this work, the breakthrough curves were obtained under various experimental conditions (Table 5) and the corresponding results are shown in Figs. 6 and 7 together with the predicted curves based on the proposed model. Fig. 6 shows the effect of temperature and pH on the adsorption breakthrough curve at different temperatures (298.15, 313.15 and 323.15 K) and pH (3 and 8). As expected from adsorption isotherms (Fig. 2a and b), the breakthrough time (i.e., adsorp-

Table 5
Experimental condition in dynamic adsorption experiments

Run	Temperature (K)	pH	L (cm)	F (mL/min)	C ₀ (mg/L)
Fix-1	298.15	8	16	2	7.35
Fix-2	313.15	8	16	2	7.35
Fix-3	323.15	8	16	2	7.35
Fix-4	298.15	3	16	2	7.35
Fix-5	298.15	8	16	2	14.7
Fix-6	298.15	8	16	4	14.7
Fix-7	298.15	8	16	8	14.7
Fix-8	298.15	8	25	2	7.35

tion amount) was higher for higher temperature and lower pH. In especial, the adsorption breakthrough curves were highly sensible to the variation of solution pH. Further studies on the effect of solution pH will be continued systematically.

Fig. 7 illustrates the effect of input concentration (7.4 and 14.7 mg/L), flow rate (2, 4 and 8 mL/min) and column length (16 and 25 cm) on the adsorption breakthrough curves. The break-time for the higher input concentration is earlier than that for the lower input concentration. The result can be explained by the concept of the moving velocity of the mass transfer zone (MTZ) [7,16,17], V_{mtz} , defined as

$$V_{mtz} = \left[\frac{\partial z}{\partial t} \right]_c = - \frac{(\partial C / \partial t)_z}{(\partial C / \partial z)_t} = \frac{v}{1 + \rho_p((1 - \varepsilon_b) / \varepsilon_b)(dq/dC)_c} \quad (14)$$

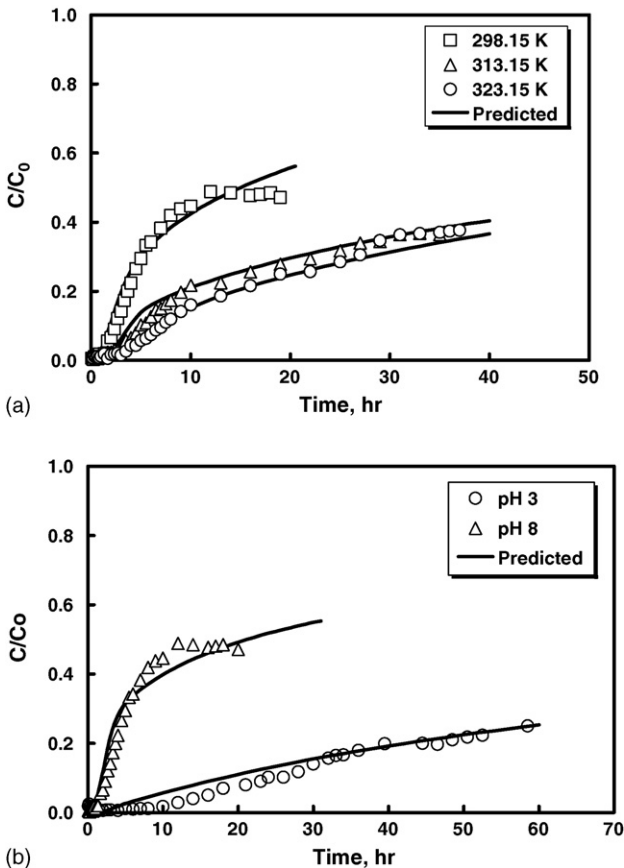


Fig. 6. Adsorption breakthrough curves of TNT in terms of temperature and pH (Fix-1, -2, -3 and -4).

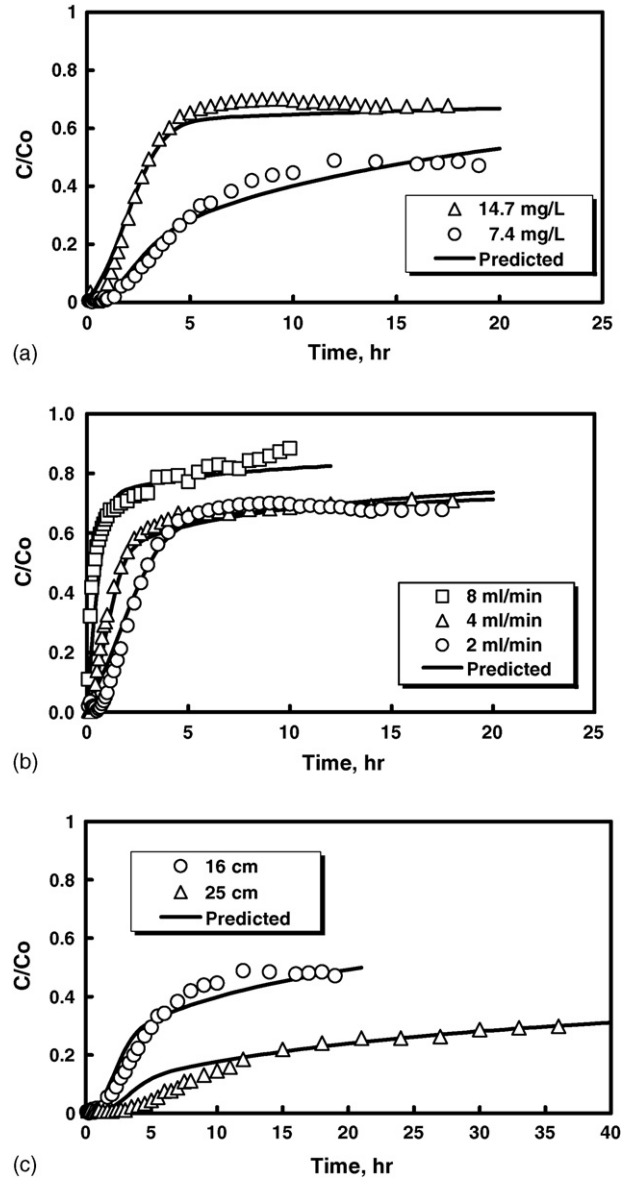


Fig. 7. Adsorption breakthrough curves of TNT in terms of: (a) concentration, (b) flow rate, and (c) column length. (Fix-5, -6, -7, and -8).

Eq. (14) means that MTZ is a function of interstitial velocity (v), particle density (ρ_p), bed porosity (ε_b) and dq/dC . For a linear isotherm adsorption system, the values of dq/dC is constant with other fixed variables, so that the moving velocity of the MTZ is constant. Therefore, the breaktime is not affected by input concentrations. However, the adsorption isotherm of TNT on activated carbon is nonlinear and weakly favorable (Fig. 2). As the input concentration increases, the value of dq/dC decreases (i.e., the zone velocity increases). Therefore, the breaktime becomes shorter under this circumstance. Fig. 7b shows that the breaktime appeared earlier with a higher flow rate. The breakthrough curves were steeper with a higher flow rate. Since the intraparticle diffusivity is usually independent of the flow rate, this was caused by the external film mass transfer resistance. This resistance is smaller when the flow rate is higher, so that the length of the mass transfer zone is reduced or a sharper breakthrough

curve is generated. When all the other operating conditions were fixed, the breakthrough curves at different column lengths were almost similar (Fig. 7c). On the basis of the experimental and theoretical results, the proposed adsorption dynamic model was successfully applied for the simulation of the general features of TNT in activated carbon column. These findings led us to conclude that the results obtained in this study may be useful in column design, scale-up, and optimization required for direct separation of TNT from the aqueous solution.

5. Conclusions

For a separation method for TNT dissolved in aqueous solutions, the adsorption equilibrium, the kinetics and the column dynamics of TNT were investigated using granular activated carbon. Adsorption isotherm data in terms of temperature and pH were well fitted by Langmuir equation. In addition, the adsorption capacity increased with increasing temperature and decreasing pH. Contrary to our expectation, the adsorption of TNT on activated carbon showed nearly homogenous adsorption properties based on the results of the shape and intensity of adsorption energy distribution calculated by the generalized nonlinear regularization method. The formulated adsorption dynamic model, which employs the surface diffusion mechanism, successfully simulated the breakthrough curves obtained under key operating conditions such as temperature, pH, concentration, flow rate, and column length. It is especially interesting that the effect of solution pH on both adsorption capacity and breakthrough curves was considerably high. Therefore, further studies on pH effect are systematically underway to remove TNT effectively.

Acknowledgements

This work was supported by the ministry of Commerce, Industry and Energy (MOCIE) through the project of Regional Innovation Center (RIC).

References

- [1] V. Marinovic, M. Ristic, M. Dostanic, *J. Hazard. Mater.* B117 (2005) 121.
- [2] C. Rajagopal, J.C. Kapoor, *J. Hazard. Mater.* B 87 (2001) 73.
- [3] R. Alnizy, A. Akgerman, *Water Res.* 33 (1999) 2021.
- [4] C.K. Scheck, F.H. Frimmel, *Water Res.* 33 (1995) 2346.
- [5] N.J. Duijm, F. Markert, *J. Hazard. Mater.* A 90 (2002) 137.
- [6] G. Muralidharan, A. Wig, L.A. Pinnaduwege, D. Hedden, T. Thundat, R.T. Lareau, *Ultramicroscopy* 97 (2003) 433.
- [7] D.M. Ruthven, *Principles of Adsorption and Adsorption Processes*, John Wiley & Sons, New York, 1984.
- [8] R.T. Yang, *Gas Separation by Adsorption Processes*, Butterworths, Boston, 1986.
- [9] J.W. Lee, H.J. Jung, D.H. Kwak, P.G. Chung, *Water Res.* 39 (2005) 617.
- [10] W. Rudzinski, D. Everett, *Adsorption of Gases on Heterogeneous Solid Surfaces*, Academic Press, London, 1991.
- [11] M. Jaroniec, R. Madey, *Physical Adsorption on Heterogeneous Solids*, Elsevier, Amsterdam, 1988.
- [12] P. Podkoscielny, A. Dabrowski, O.K. Marjuk, *Appl. Surf. Sci.* 205 (2003) 297.
- [13] J. Villadsen, M.L. Michelsen, *Solution of Differential Equation Models by Polynomial Approximation*, Prentice-Hall, New Jersey, 1978.
- [14] J.W. Lee, T.O. Kwon, I.S. Moon, *Carbon* 42 (2004) 371.
- [15] R.C. Reid, J.M. Prausnitz, B.E. Poling, *The Properties of Gases and Liquids*, McGraw-Hill, New York, 1994.
- [16] J.W. Lee, H.C. Park, H. Moon, *Sep. Purif. Technol.* 12 (1997) 1.
- [17] J.W. Lee, H. Moon, *Adsorption* 5 (1999) 381.